Sensors and Actuators A 318 (2021) 112532

Contents lists available at ScienceDirect

Sensors and Actuators A: Physical

journal homepage: www.elsevier.com/locate/sna

Piezoresistive electronic skin based on diverse bionic microstructure

Hao Tang[a,b], Pu Nie[a,b], Ranran Wang[a,c,*], Jing Sun[a]

[a] State Key Laboratory of High Performance Ceramics and Superfine Microstructure, Shanghai Institute of Ceramics, Chinese Academy of Sciences, Shanghai, 200050, China
[b] University of Chinese Academy of Sciences, 19 Yuquan Road, Beijing, 100049, China
[c] School of Chemistry and Materials Science, Hangzhou Institute for Advanced Study, University of Chinese Academy of Sciences, 1 Sub-Lane Xiangshan, Hangzhou, 310024, China

ARTICLE INFO

Article history:
Received 30 September 2020
Received in revised form
23 December 2020
Accepted 30 December 2020
Available online 4 January 2021

Keywords:
Electronic skin
Microstructure
Crack
Bionic
Plant leaf

ABSTRACT

With the introduction of micro nano structure, the performance of electronic skin (E-skin), as a flexible pressure sensor, has been significantly improved. However, most of the pre templates for constructing micro nano structure are fabricated by photolithography, which endows them with the limitation of surface microstructure and the difficulty of forming complex multi-level structures. Distinguished from the artificial micro-structured silicon template, there are abundant microstructure distributed on the surface of natural plant leaves for us to choose. The diversity of plant leaves provides more possibility for us to explore the internal relationship between the microstructure distributed on electrode surface and the performance of E-skin device. Herein, four kinds of plant leaves are selected as templates to fabricate E-skins with different bionic microstructures. The various sensing performances of four kinds of devices are evaluated through the real-time monitoring of current signal, and the device based on nerium oleander template exhibits the most outstanding performance (sensing range: 0–0.8 kPa, sensitivity: 8.5 kPa^{-1}, detection limit: 0.001 kPa). Furthermore, quantitative indicators (radius/height and density) for the surface microstructure of E-skin are proposed to explain the performance differences between these devices. The device with fine (small values of radius/height) and high-density microstructure trends to exhibit high sensitivity and low detection limit as well as good durability. Additionally, the activating phenomenon of the E-skin during repeated compression was observed and the underlying mechanism was discussed. Finally, the E-skin based on nerium oleander template has been successfully employed to detect the subtle distinction of physiological signals in a series of fitness actions.

1. Introduction

With the recent advances in intelligent terminal and robot, people put forward higher requirements for electronic devices that are more flexible and wearable. E-skin, as a branch of flexible devices, plays a significant role in human-computer interface and has attracted great interest of researchers all over the world [1–6]. Human skin, as the largest organ of human body, is able to sense many kinds of external signals and transmit them to cerebral cortex [7–9]. Similarly, E-skin is also capable of sensing external signals like human skin, such as stress, temperature and humidity, which is even beyond the perceptual limit of human skin in the identification of tiny signals and the response range. In light of that, E-skin shows exceptional promise in the field of health monitoring, motion sensing and artificial intelligence [10–14]. The development of E-skin will undoubtedly promote revolutionary progress in various fields and improve people's quality of life.

Flexible pressure sensor is an important module for external stress sensing of E-skin, which has attracted extensive attention and study. The performance metrics of flexible pressure sensor mainly consist of sensitivity, linear detection range, hysteresis response, detection limit, response time and durability, along with the stability in corrosive environment [11,14]. In all kinds of flexible of pressure sensors [15–23], the sensor based on piezoresistive mechanism have been widely investigated because it offers high sensitivity in low pressure zone, relatively simple components, and a low detection limit [24,25]. Resistive pressure sensor is assembled of two parts: one is conductive layer, which mainly employs carbon nanotubes, graphene, metal nanowires and other conductive materials. Another is elastic substance, on which some microstructures are formed, including sponges [26], pyramidal structure [8,27],

* Corresponding author at: State Key Laboratory of High Performance Ceramics and Superfine Microstructure, Shanghai Institute of Ceramics, Chinese Academy of Sciences, Shanghai, 200050, China.
E-mail address: wangranran@mail.sic.ac.cn (R. Wang).

https://doi.org/10.1016/j.sna.2020.112532
0924-4247/

nanofiber [28] and reverse-dome [17]. The micropattern formed on the surface of elastic substance is aimed at adjusting the elastic modulus and reducing shape factor [27], enabling the easy deformation and concentrated stress, so that the performance of flexible pressure sensor could be tremendously improved. For instance, following the classic pyramid structure constructed on PDMS surface reported by Bao's team [19,29,30], which endowed E-skin with high sensitivity and short response time, a series of devices based on diverse microstructure emerged. The pressure sensor with a novel hierarchical structure in Bae's study [17] exhibited high sensitivity (8.5 kPa^{-1}) in a wide linear detection range (up to 12 kPa). The approach of fabricating these micro-structured elastic substrates in above literatures is to reproduce the microstructure of patterned silicon template, which is obtained by high time consuming and cost photolithography process. Besides, this kind of artificial template is difficult to realize the processing of complex microstructure and is limited by the designer's ideas. Therefore, researchers try to find a cheaper and more efficient method to fabricate the elastic substrate with microstructure. There are abundant microstructures distributed on the surface of plant leaves, which is the result of natural selection after a long- term evolution. As a simple and efficient approach, the direct or inverted microstructures of many plant leaves have been employed to fabricate high-performance E-skin in previous studies, such as mimosa [31], rose petal [32] and banana leaf [33]. However, the surface microstructures reported in these works varied significantly from each other. It is difficult to form a contrast between various microstructure and to distinguish the inherent correlation between microstructures and the sensing performance.

This paper is devoted to explore the influence trend of different bionic microstructures on the performances of E-skin and try to find some regularity, thus providing theoretical guidance for the preparation of high-performance E-skin. Four kinds of plant leaves with regular changes on surface microstructure were used as templates to prepare micropatterned flexible electrodes. E-skins with tunable sensitivity and detection range have been fabricated based on these electrodes. The correlation between the surface microstructure and the performance of E-skin was thoroughly investigated. When the typical parameters (radius/height: the ratio of bottom radius to bulge height of single microstructure unit on elastic substrate) is 1.5, the E-skin exhibits 8.5 kPa^{-1} in sensitivity and detection limit as low as 0.001 kPa as well as good cycling stability, which endow it with great potential to achieve timely and reliable pressure monitoring. The E-skin based on nerium oleander template, which has the best sensing performance among the four devices, was employed to monitor the subtle changes of muscles in vocal cord vibration and fitness movement, making it possible to provide professional guidance for vocalization and fitness through wearable devices.

2. Result and discussion

The schematic illustration of bioinspired flexible pressure sensor manufacturing is shown in Fig. 1a. Leaves of four plants with typical microstructure were selected to fabricate micropatterned PDMS films. For obtaining intact PDMS films, the mixture of prepolymer and curing agent was filled into the templates and bubbles were completely removed. After solidification, the PDMS films with the inverted microstructure of thalia dealbata and asplenium antiquum were accomplished, whose surface micropattern consists of many bulges. In order to ensure the comparability between the performances of four kinds of E-skins, the PDMS films with the inverted microstructure of nerium oleander and cercis chinensis, which have sunken micropatterns, were copied again as negative templates to obtain PDMS films with convex micropattern. Scanning electron microscope was employed to observe the microstructure formed on PDMS films surface. As shown in Fig. 1b–e, PDMS films made from the four templates are all featured with protuberant microstructures on micrometer scale and the structures are relatively regular. The thalia dealbata templated PDMS film exhibits numerous circular bulges distributed in interval (diameter: ~30 μm, height: ~6.0 μm, Fig. 1b), and a series of smaller protuberance (diameter: ~18 μm height: ~6.0 μm, Fig. 1c) covers the surface of nerium oleander templated PDMS film. The protuberances in the cercis chinensis templated PDMS film exhibit the planar size of around 32 μm and the height of about 4.0 μm, which are less cuspidal than the structures in nerium oleander templated PDMS film. The asplenium antiquum templated PDMS film shows a more gradual surface micropattern. The planar size of the microstructure is about 25 μm and the height is about 2.5 μm, as shown in Fig. 1e. The uniform distribution of microstructure ensures the good repeatability of E-skin device and stable sensing performance.

Following the previous study, silver coating with the thickness of 50 nm was deposited on the micropatterned PDMS films for maintaining the bionic structures and providing adequate electron transport capability. Additionally, it is not difficult to indicate from the date in Table 1 that the surface resistance of flexible electrode will get an increase when the microstructure is introduced. The E-skin devices were assembled by two flexible electrodes, one of which had a rough surface obtained from different plant templates, and the other possessed a flat surface. The external pressure was concentrated on small areas through the microstructure distributed on PDMS film, which was responsible for the great change of resistance under low pressure. The rough-to-flat surfaces interlocked E-skin device was investigated in order to better analyze the function of different microstructure on sensing performance.

According to the previous studies of Bao's group [19], a glass slide that entirely covered the device was employed to prevent the external stress from concentrating on the probe of dynamometer and provide a "base pressure" for the E-skin. With the continuous monitoring of sensor current and applied pressure, the real-time sensitivity of the E-skins with different interfacial microstructures were obtained. The sensitivity S is defined as the ratio of $\Delta(\frac{I-I_0}{I_0})$ and $\Delta\ \frac{F}{A}$, where I is the real-time current of E-skin under applied pressure, I_0 corresponds to the initial current of E-skin under base pressure, F is the external load, and A represents the contact area of two flexible electrodes.

As mentioned in previous studies, the resultant resistance (R) of E-skin consists of three parts: the resistance of top electrode (R_{TE}), contact interface (R_{CI}), and bottom electrode (R_{BE}). For studying the influence of microstructure on the sensitivity of E-skin, response curves of the four devices, which have reproduced the inverted microstructure of thalia dealbata, nerium oleander, cercis chinensis and asplenium antiquum respectively, are compared in Fig. 2a–d. And the working principle of these devices is shown in Fig. S1. It is obvious that the response curves of four kinds of E-skin are all composed of two linear response regions. In the first stage, the sensitivity is very high but the response range is narrow, while the second stage exhibits the opposite performance (low sensitivity but wide response range). In addition, the above two performance indicators of the four kinds of devices differ greatly from each other, which is mainly determined by the diverse microstructures distributed on the surface of flexible electrodes.

The highest sensitivity in the low pressure zone appeared in the E-skin based on nerium oleander template, which also had the minimum linear detection range (S = 8.5 kPa^{-1}, 0–0.8 kPa). The two

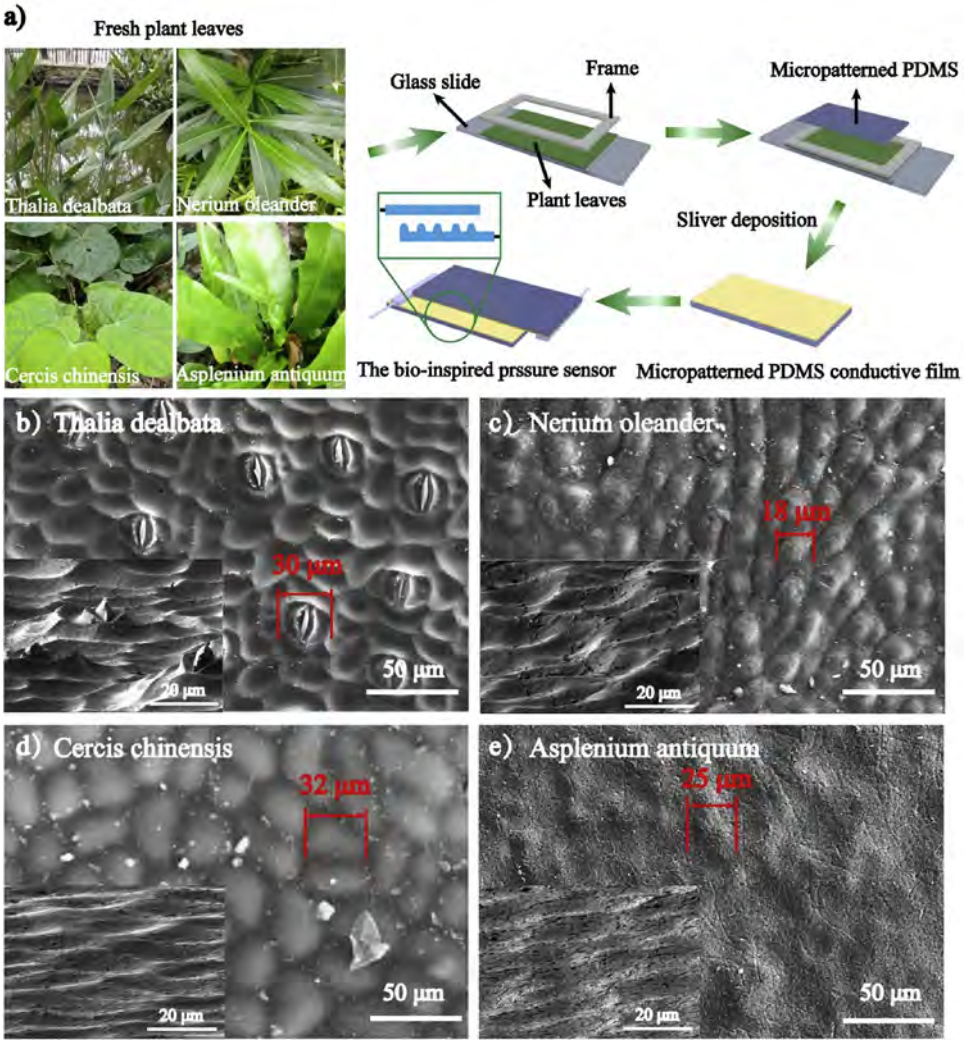

Fig. 1. (a) Fabrication process for the bioinspired flexible pressure sensors based on four different plant leaves. (b-e) Top-view SEM images of conductive PDMS electrodes with the inverted microstructure of thalia dealbata, nerium oleander, cercis chinensis and asplenium antiquum, respectively. These insets located in the lower left corner are the SEM images of surface bulge with 10° tilt angle.

Table 1
Surface resistance of flexible electrode with different plant templates.

Template	Thalia dealbata	Nerium oleander	Cercis chinensis	Asplenium antiquum	Slide glass
radius/height	15 μm/6 μm	9 μm/6 μm	16 μm/4 μm	12.5 μm/2.5 μm	–
Resistance	35 Ω sq^{-1}	60 Ω sq^{-1}	100 Ω sq^{-1}	45 Ω sq^{-1}	10 Ω sq^{-1}

performance indicators of E-skin based on asplenium antiquum template were exactly the opposite

(S = 0.5 kPa^{-1}, 0–3 kPa). The other two devices are similar in both sensitivity and linear detection range. In order to validate the efficacy of micro-structured surface on the performance of E-skins device, two flexible electrodes with flat surface were bonded together to conduct pressure sensing test. According to the result given in Fig. S2, the pressure response curve of control sample is also divided into two stages, and the sensitivity of both stages is lower than that of the sample with surface microstructure. Among them, the sensitivity difference of the second stage is more obvious because the gap between these two flat electrodes almost disappeared in the large pressure zone, which cannot provide more deformation space for further increasing pressure.

In view of the relatively regular shape of the surface bulge, we introduce the ratio of radius to height (r/h) as a typical parameter, so as to directly reveal the relationship between microstructure and sensitivity in low pressure zone. According to the SEM images of flexible PDMS electrodes with different templates (Fig. 1b–e), the order of the ratio of radius to height (r/h) is Nerium oleander template (9 μm/6 μm = 1.5) < Cercis chinensis template (16 μm/4 μm = 4) < Asplenium antiquum template (12.5 μm/2.5 μm = 5). For these three samples, the lower the ratio of radius to height (r/h), the higher the sensitivity in the low pressure zone. Following the above rules, the sensitivity of the device based on thalia dealbata template (15 μm/6 μm = 2.5) should be in the range of 2.88–8.5 kPa^{-1}, while it was actually measured to be 2.75 kPa^{-1}. This phenomenon is attributed to the smaller distribution density of effective micropattern, on account of which fewer contact sites were offered during external loading. On the other hand, the rank of linear detection range is Nerium oleander template (0–0.8 kPa) < Cercis chinensis template (0–2.6 kPa) < Asplenium antiquum template (0–3 kPa), which is exactly opposite to the order of sensitivity, indicating the trade off between

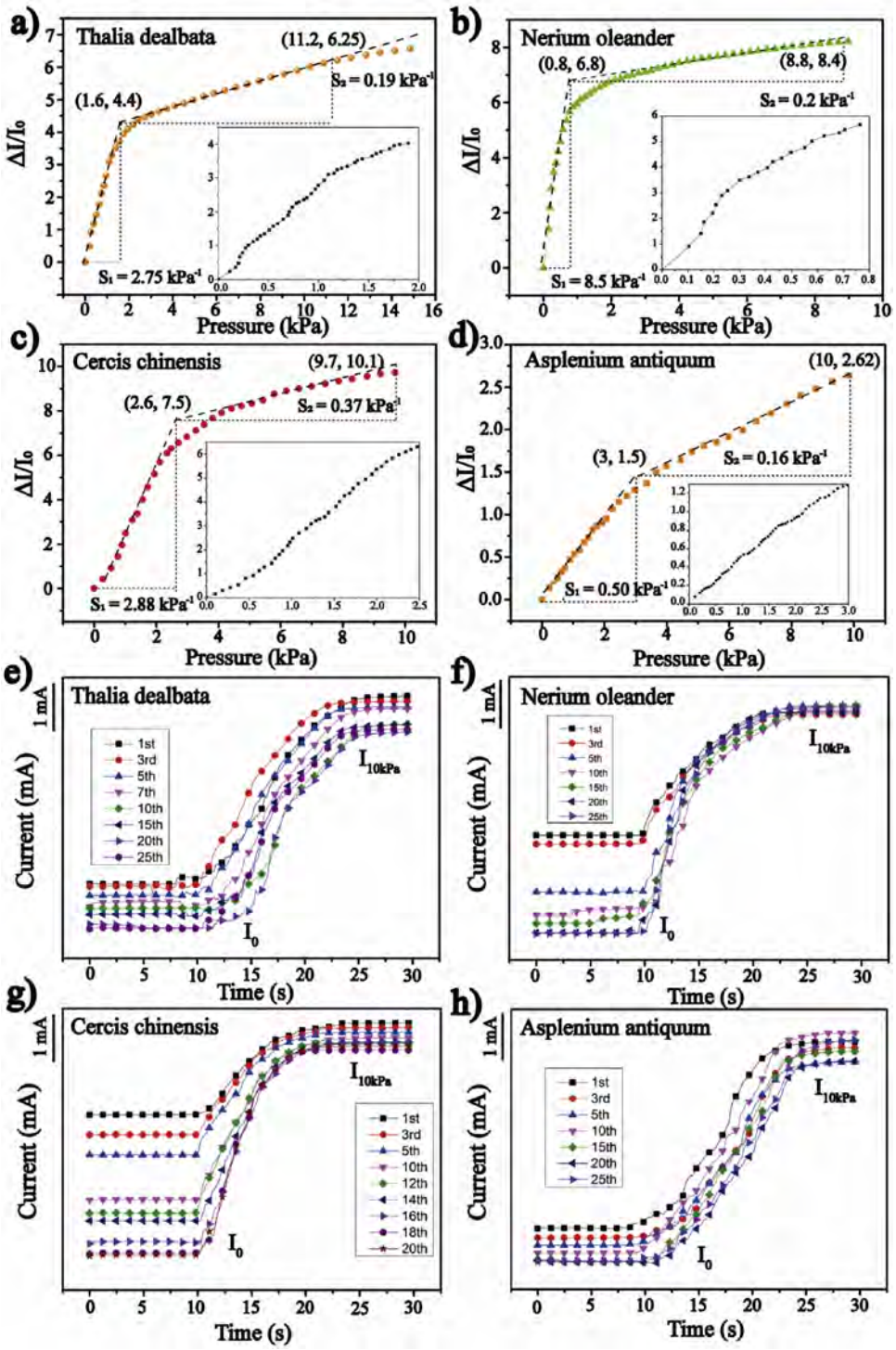

Fig. 2. Relative current variation-pressure curves of the E-skin based on four different microstructure templates in the first compression: (a) Thalia dealbata template; (b) Nerium oleander template; (c) Cercis chinensis template; (d) Asplenium antiquum template. The insets correspond to the amplification of the current variation-pressure curves in the first stage of four kinds of E-skin devices. Current-time curves of the E-skin devices based on four different microstructure templates in multiple compression (pressure: 0–10 kPa): (e) Thalia dealbata template; (f) Nerium oleander template; (g) Cercis chinensis template; (h) Asplenium antiquum template.

the sensitivity and linear detection range of these devices. Based on the above analysis, it can be concluded that microstructures with small value of r/h generally lead to higher sensitivity and narrower linear detection range, and vice versa. Sensitivity and linear detection range are mutually restricted for a single microstructure, and constructing multi-level microstructure should be an effective approach to obtain high sensitivity and wider linear range of E-skin devices simultaneously.

We continuously tested the sensitivity of four kinds of E-skin devices based on different plant templates for more than 20 times, and the curve of current and time are shown in Fig. 2e–h. With the increase of test times, the initial current of these E-skins experienced a process of gradually decreasing and eventually maintaining stable, which was consistent with the results reported in previous literature [33]. Our previous work has indicated that the variation of initial current is attributed to the appearance, proliferation and sat-

uration of microcracks on the surface of flexible electrode. After the first cycle of compression, many tiny cracks appear in the sliver conductive layer, which results in irreversible increase of resistance. The cracks propagate and then reach saturation after several tenth cycles. We name this process the activation process, after which the sensor can work more stably. Comparing the initial current reduction of four kinds of E-skins based on different plant templates, both nerium oleander template and cercis chinensis template have a significant change. The former reduced by 75 %, while the latter had 90 % drop. By contrast, the E-skins based on thalia dealbata template and asplenium antiquum template have a small change in initial current, which reduced by 58 % and 33 %, respectively. The reason for the difference in the variation of initial current is the diverse proportion of the saturated crack area on the surface of flexible electrodes with four kinds of plant templates. What is shown in Fig. S3 is that the microcracks distributed on the surface of flexible electrode, and it is obvious that the crack density of the E-skins based on nerium oleander template and cercis chinensis template is higher than those based on thalia dealbata template and asplenium antiquum template. Additionally, statistical software was employed to identify the proportion of saturated crack area in the above SEM photos, whose straightforward numerical result is provided in Fig. S4. Specifically, it is 0.11785 for thalia dealbata template, 0.20534 for nerium oleander template, 0.24054 for cercis chinensis, and 0.11956 for asplenium antiquum. The E- skins with fine (small values of r/h) and high-density surface microstructure, such as nerium oleander and cercis chinensis templated ones, are more likely to deform when the external load is applied. And the silver conducting layer on the surface of flexible electrode is damaged greatly, which lead to a large proportion of saturated crack area andan obvious reduction of initial current. Another interesting phenomenon is that the variation of final saturation current (Current at 10 kPa) is also closely related to the microstructure distributed on the surface of flexible electrode. The fine (small values of r/h) and high-density microstructure is also able to make the device undergo large deformation under high pressure, which can drive more cracks to coalesce, so that the reduction of saturation current is relatively small. For E-skins based on nerium oleander and cercis chinensis, the initial current decreases significantly, while the saturated current is relatively stable, which means that the device's sensitivity constantly increased until a stable value during the first several tenth cycles. This process is defined as the activation process, which is believed to be a common phenomenon. By adjusting the surface microstructure of flexible electrode, the variation of initial current and saturated current during repeated compression can be controlled, thus ameliorating the current-pressure response characteristics of E-skin device.

To further compare the capability of E-skins based on different plant templates to perceive tiny pressure, the detection limit curve of these flexible piezoresistive sensors were investigated and shown in Fig. 3a. The result indicates that the detection limit of E-skin based on nerium oleander template is the lowest, which can accurately reflect the load of 0.001 kPa. The detection limits of E-skin based on thalia dealbata and cercis chinensis template are 0.002 kPa and 0.004 kPa respectively. For the device based on asplenium antiquum, notable signal only arises when the external load reaches 0.01 kPa. The trend is in accordance with that of sensitivity of the four kind of E-skins, which can be ascribed to the different ratio of radius to height (r/h) of the interfacial microstructures.

Fig. 3b compares the response and relaxation time of E-skins based on four kinds of plant templates. With a pressure of 1 kPa loading or unloading from the surface of device, the response and relaxation time of E-skins based on four kinds of plant templates are 40–50 ms, which is comparative to that of human skin [35]. As previously reported, the construction of surface microstructure greatly suppressed the inherent viscoelasticity of PDMS, thus make it possible to produce E-skin with short response time.

The durability of four E-skins based on different plant templates is demonstrated in Fig. 3c. Each device was tested for 5000 cycles of 1 kPa loading/unloading (0.4 Hz), and the current change of the first

200 cycles in every 1000 cycles were plotted. Part of the current curve after 4000 cycles is amplified and provided in the right image of Fig. 3c. These curves show that there is no obvious degradation in the response signal after 4000 cycles, because the number of cracks distributed in silver conductive layer had all reached saturation state for the four kinds of E-skin. Additionally, the hysteresis response of the device based on nerium oleander template is provided in Fig. S5. According to the formula $\text{Hysteresis}(\%) = \left|\frac{Y_{load}-Y_{unload}}{Y_{max}-Y_{min}}\right| \cdot 100\%$ [34], where Y_{load} - Y_{unload} is the greatest difference of $\Delta I/I_0$ during loading and unloading response, and the Y_{max} and Y_{min} represent the value of $\Delta I/I_0$ at maximum and minimum loading, the hysteresis of the device based on nerium oleander template was calculated to be 13.1 %.

The construction of bionic microstructures endows E-skin with enhanced sensing performance, so that accurate detection of human activities can be achieved by this device. Such an E-skin (Nerium oleander template) was attached to a volunteer's throat for monitoring the vibration of vocal cords (Fig. 4a). As shown in Fig. 4b, c, the E-skin is capable of distinguishing different words and stress syllable exactly, such as "Magic", "Science", "Philosophy" and "History". In addition, the current signal emerges copied shapes when the same word was said, which demonstrates the good repeatability of this device. The flexible device is a potential candidate for pronunciation correction and speech recognition.

Besides, the E-skin can also be employed to detect muscle contraction under different loads. When the E-skin based on nerium oleander templates was mounted on the biceps brachii, the subtle differences in muscle contraction under different loads can be identified and precisely displayed in the current curve (Fig. 4d). The loads in Fig. 4d are 0 kg (natural grip), 3 kg and 6 kg respectively, and it is obvious that the change of current intensity is not linear with load increment, which is attributed to that the contraction of biceps brachii becomes more and more difficult with the increase of load. Besides, there are two peaks of current signal in one elbow flexion cycle, which correspond to two peak contraction of biceps brachii. The two peak contractions of biceps brachii are almost the same without external loading (The current intensity are similar). In the case of heavy loading (3 kg, 6 kg), however, the second current peak is relatively high, indicating that the muscle contracted more tightly when the dumbbell was put down than when the dumbbells was raised. Similarly, as shown in Fig. 4e, the E-skin stuck on the triceps brachii was used to monitor muscle contraction under 0 kg (natural grip), 1.5 kg and 3 kg loads. In the classic training of triceps brachii, the current signal more clearly captured the two peak contractions of the muscle, and the reason why the second peak is significantly higher is consistent with the previous analysis of biceps brachii. The E-skin also successfully distinguished the contraction of biceps femoris (Fig. 4f) under different loads. However, unlike the arm muscles, the thigh muscles bear the external loading, while they also support the weight of upper body, which cannot be ignored. During one cycle of squat, the sharp peaks of current signal at the beginning and ending were detected by the E-skin, which were caused by the activation and braking of thigh muscles for upper body. At other times, the contraction of biceps femoris is similar to that of arm muscles.

Moreover, as an effective method of training core muscles, planking is very popular among fitness enthusiasts (Fig. 4g). The E-skin was attached to the abdomen of volunteers to monitor the breathing condition during planking process in real time, and

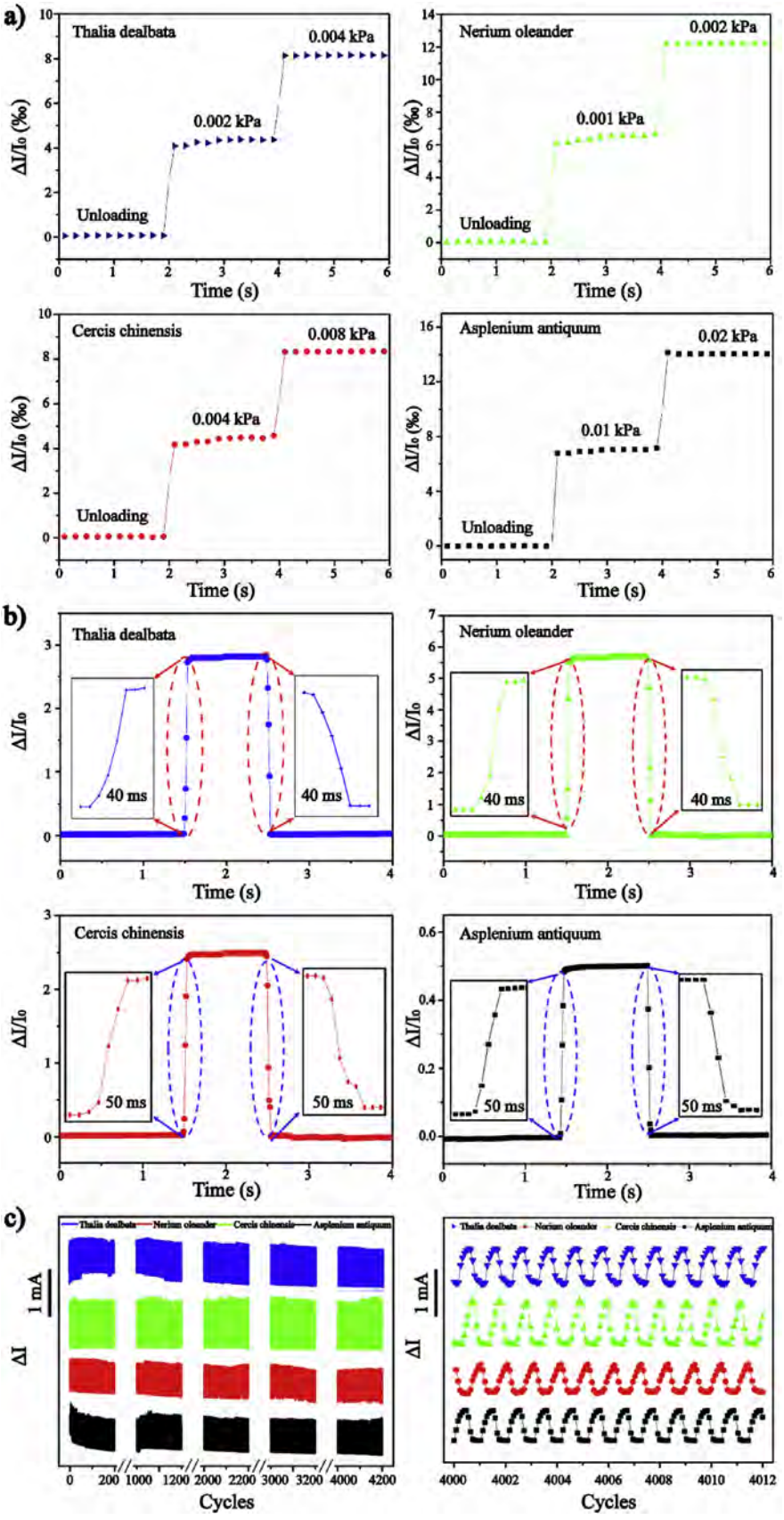

Fig. 3. (a) Detection limit, (b) response time and (c) cycling durability of the E-skin devices based on four different microstructure templates.

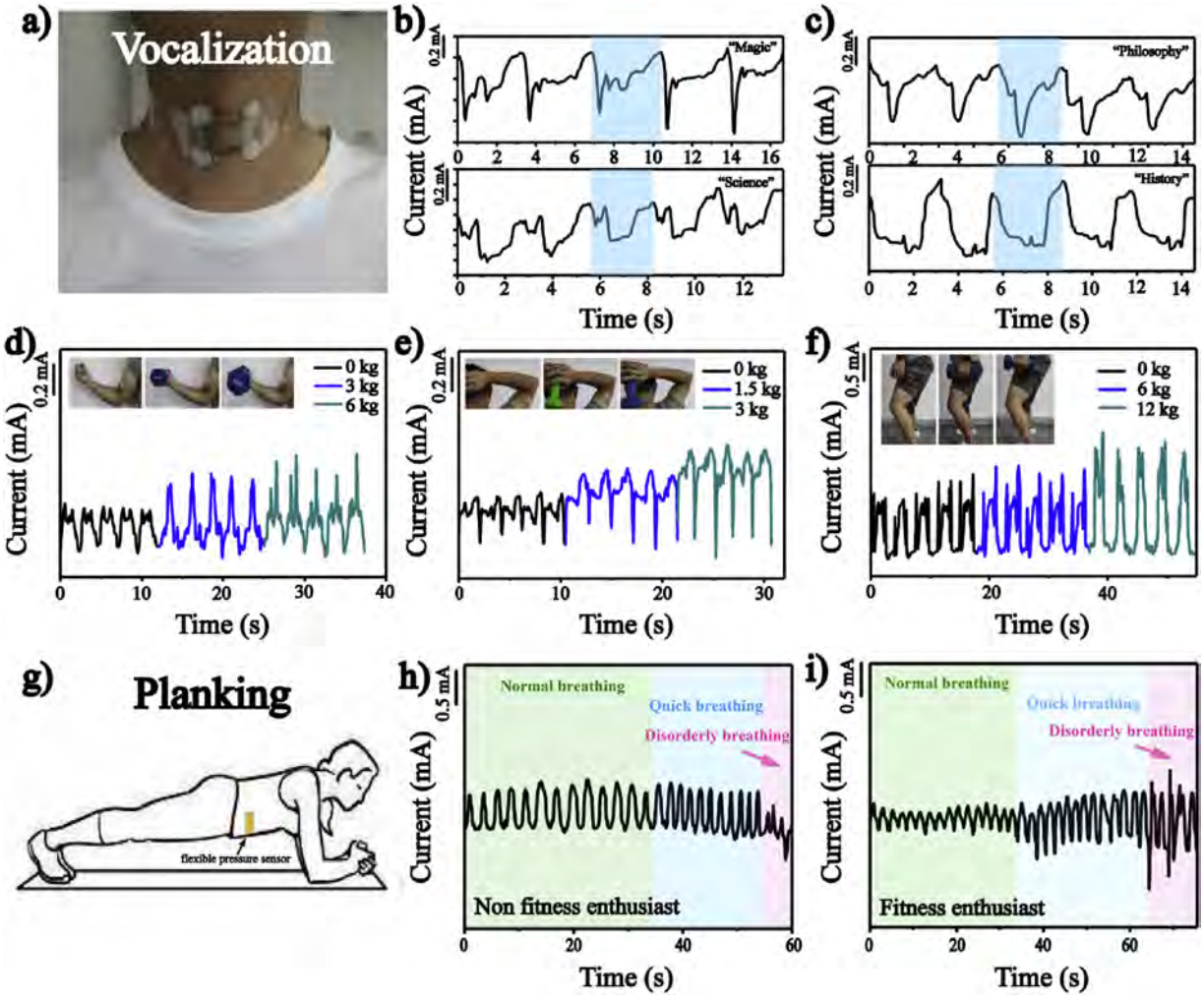

Fig. 4. Monitoring of vocalization, muscle contraction and breathing condition with the E-skin devices (Nerium oleander template). (a) The E-skin attached to a volunteer's neck for monitoring the vibration of vocal cords. (b, c) Current-time curves of the E-skin devices corresponding to different words: "Magic", "Science", "Philosophy" and "History". (d) Monitoring the contraction of biceps brachii when the weight-bearing is 0 kg, 3 kg and 6 kg, respectively. (e) Monitoring the contraction of triceps brachii when the weight-bearing is 0 kg, 1.5 kg and 3 kg, respectively. (f) Monitoring the contraction of biceps femoris when the weight-bearing is 0 kg, 6 kg and 12 kg, respectively. (g) Standard posture of planking. The E-skin was attached to the abdomen of volunteers' body. (h, i) Comparison of breathing condition between non fitness enthusiast and fitness enthusiast during planking. Breathing condition was divided into three stages: normal breathing, quick breathing and disorderly breathing.

the breathing process can be divided into three significant stages, including normal breathing, quick breathing and disorderly breathing. By comparing the breathing of non-fitness enthusiasts and fitness enthusiasts during planking, whose results are shown in Fig. 4h, i, it is obvious that the latter maintains the action for a longer time (75 s for fitness enthusiasts >60 s for non-fitness enthusiasts). Additionally, in the normal breathing stage, the fitness enthusiast is more relaxed than the other, because his breathing is shallower and closer to inactivity. In the stage of quick breathing, the respiratory rate and amplitude of both volunteers are increased. In the final stage, fitness enthusiast is still able to basically maintain the stability of breathing, while the breathing of non-fitness enthusiast has completely lost its regularity. Along these lines, the E-skin would provide a very convenient way to achieve the monitoring of body function, perhaps enabling the professional guidance for fitness.

In addition, wearable electronic devices also put forward high requirement for the waterproof of materials (the interference on device's accuracy come from sweat) and long-term stability. The water contact angles were tested to evaluate the water proof ability of flexible electrodes with microstructure and flat surface, which are shown in Fig. S6. The maximum contact angle appears on the surface of flat silver electrode (98°). With the introduction of surface microstructure, the contact angle decreases slightly, while it still remains above 80°, indicating that these E-skin devices are relatively not easy to be wetted by sweat or ambient moisture. Furthermore, the packaging of E-skin device with silicone rubber is able to completely shield the influence of humid environment, and the aging results of devices with and without packaged at 100 % humidity are shown in Fig. S7. The resistance of the conductive sliver layer increased gradually in the long-term contact with 100 % humidity environment (1.35 times change within 48 h). However, the package of device by silicone rubber is capable of achieving the good stability (almost no change in 48 h), which provides an effective way for the stable output of wearable E-skin devices. Besides, we also tested the relative resistance change of E-skin devices placed in atmospheric environment for one week (Fig. S8), and the aging phenomenon was not obvious whether the devices were packaged or not.

3. Conclusions

We have fabricated piezoresistive flexible pressure sensors based on the microstructure of thalia dealbata, nerium oleander,

cercis chinensis and asplenium antiquum, respectively. According to the comparative analysis of microstructure and the sensitivity curve, the relationship between typical parameters r/h and the performance of E-skin was discovered. Specifically, the E-skin device with fine (small values of r/h) and high-density interfacial microstructure has high sensitivity, low detection limit, better durability but narrow linear range. The introduction of microstructure not only facilitate the deformation of the flexible electrodes, which leads to dramatic changes in contact resistance, but also affects the crack and coalescence behavior of the conducting layer. The E-skin based on nerium oleander template realizes the subtle recognition of some fitness actions. More importantly, this work can provide some guidance for the structure design of E-skin, so that higher performance can be achieved.

4. Experimental section

4.1. Fabrication of micropatterned PDMS conductive film

First of all, large leaves were selected and thick veins were avoided in order to maintain the integrity and repeatability of templates. Different plant leaves were cut into the proper size and washed with deionized water and ethanol. After drying with a blower, clean plant leaves were obtained and attached to glass slides. Additionally, double faced adhesive tape was employed to ensure the flat combination between leaves and glass.

Next, the PDMS prepolymer and curing agent was mixed in a weight ratio of 10 to 1 (Dow Corning Sylgard 184) and stirred for 10 min. The mixture was poured into the frame (30 mm * 15 mm * 0.25 mm) and placed in vacuum environment for removing the bubbles. Besides, vacuum environment also helped the liquid fill the remaining space to accurately reproduce the microstructure on plant leaves. Next, another slide was pressed on the surface of frame to extrude the excess PDMS liquid, and it was fixed by clamps. The liquids limited in rectangular frame were transformed into micropatterned PDMS film after being treated at 80 °C for 4 h. Smooth glass slide was exploited to fabrication flat PDMS film. It is noteworthy that the first obtained PDMS films with nerium oleander and cercis chinensis templates were used as negative template to produce positive template PDMS films through the same method again, which are covered by raised surface microstructure. The release agent (an oily substance) was sprayed on the surface of negative PDMS template to ensure that they did not stuck to each other during convex micropattern formation.

Finally, PDMS film was coated by silver coating through thermal evaporation, which did not hide the microstructure distributed on the surface of this film. And, a series of conductive PDMS films, which had different microstructure induced by plant leaves, were obtained. It is noteworthy that the flexible electrodes with nerium oleander and cercis chinensis templates was obtained by using the above method twice.

4.2. Fabrication of flexible E-skin

The flexible pressure sensor was composed of two conductive PDMS films placed face-to-face, one of which replicated the microstructure on the surface of plant leaves, and the other was flat. Copper wires were connected to the edge of the conductive films with silver paste for the output of Electrical signal. And the position coated by sliver paste should be avoided when the devices were assembled. Finally, adhesive tape was employed to ensure the stable combination of two conductive PDMS films and the bioinspired flexible E-skin was generated.

4.3. Characterization

The morphologies of the conductive PDMS films with bioinspired micropattern were characterized by a field emission scanning electron microscope (S-4800, Hitachi, Japan). The resistance variation was recorded by electrochemical workstation (PARST2273, Princeton Applied Research), which loaded a constant voltage to the flexible pressure sensor and monitored real-time current. The force applied on these pressure sensors was measured by a force gauge (Handpi Digital force gauge, HP5). The pressure sensing tests were conducted by a high precision electronic universal testing machine (CMT6103, MTS Systems, China) with a software system, and the durability test was determined by a movable stage (ZXT _050-300 _MA06, China, Shanghai Zhengxin Optio-electrical Technology Co. Ltd.).

Author statement

Hao Tang and Pu Nie were mainly responsible for proposing the experimental concept and designing the experimental scheme, and then completed a series of data testing and writing work. Ranran Wang and Jing Sun mainly evaluated the scientificity of the experimental methods, and gave systematic guidance to the experimental conclusions and manuscripts.

Declaration of Competing Interest

The authors declare that they have no known competing financial interests or personal relationships that could have appeared to influence the work reported in this paper.

Acknowledgments

This work was supported by the National Natural Science Foundation of China (Grant No. 61871368), the Youth Innovation Promotion Association CAS, the Young Elite Scientists Sponsorship Program by CAST, and the Austrian-Chinese Cooperative R&D projects (GJHZ2046).

Appendix A. Supplementary data

Supplementary material related to this article can be found, in the online version, at doi:https://doi.org/10.1016/j.sna.2020.112532.

References

[1] S.H. Wang, J.Y. Oh, J. Xu, H. Tran, Z.A. Bao, Skin-Inspired Electronics: An Emerging Paradigm, Acc. Chem. Res. 51 (2018) 1033–1045.
[2] Y.H. Lee, O.Y. Kweon, H. Kim, J.H. Yoo, S.G. Han, J.H. Oh, Recent advances in organic sensors for health self-monitoring systems, J. Mater. Chem. C 6 (2018) 8569–8612.
[3] W. Gao, H. Ota, D. Kiriya, K. Takei, A. Javey, Flexible electronics toward wearable sensing, Acc. Chem. Res. 52 (2019) 523–533.
[4] T. Someya, M. Amagai, Toward a new generation of smart skins, Nat. Biotechnol. 37 (2019) 382–388.
[5] Y. Khan, A.E. Ostfeld, C.M. Lochner, A. Pierre, A.C. Arias, Monitoring of vital signs with flexible and wearable medical devices, Adv. Mater. 28 (2016) 4373–4395.
[6] T.R. Ray, J. Choi, A.J. Bandodkar, S. Krishnan, P. Gutruf, L.M. Tian, R. Ghaffari, J.A. Rogers, Bio-integrated wearable systems: a comprehensive review, Chem. Rev. 119 (2019) 5461–5533.
[7] A. Zimmerman, L. Bai, D.D. Ginty, The gentle touch receptors of mammalian skin, Science 346 (2014) 950–954.
[8] B.C.K. Tee, A. Chortos, A. Berndt, A.K. Nguyen, A. Tom, A. McGuire, Z.C. Lin, K. Tien, W.-G. Bae, H. Wang, P. Mei, H.-H. Chou, B. Cui, K. Deisseroth, T.N. Ng, Z. Bao, A skin-inspired organic digital mechanoreceptor, Science 350 (2015) 313–316.
[9] S. Raspopovic, M. Capogrosso, F.M. Petrini, M. Bonizzato, J. Rigosa, G. Di Pino, J. Carpaneto, M. Controzzi, T. Boretius, E. Fernandez, G. Granata, C.M. Oddo, L. Citi, A.L. Ciancio, C. Cipriani, M.C. Carrozza, W. Jensen, E. Guglielmelli, T.

Stieglitz, P.M. Rossini, S. Micera, Restoring natural sensory feedback in real-time bidirectional hand prostheses, Sci. Transl. Med. 6 (2014).
[10] H. Zeng, Y. Zhao, Sensing movement: microsensors for body motion measurement, Sensors 11 (2011) 638–660.
[11] M.L. Hammock, A. Chortos, B.C.K. Tee, J.B.H. Tok, Z. Bao, 25th anniversary article: the evolution of electronic skin (E-skin): a brief history, design considerations, and recent progress, Adv. Mater. 25 (2013) 5997–6037.
[12] Y. Adesida, E. Papi, A.H. McGregor, Exploring the role of wearable technology in sport kinematics and kinetics: a systematic review, Sensors 19 (2019).
[13] M. Segev-Bar, H. Haick, Flexible sensors based on nanoparticles, ACS Nano 7 (2013) 8366–8378.
[14] M. Amit, L. Chukoskie, A.J. Skalsky, H. Garudadri, T.N. Ng, Flexible pressure sensors for objective assessment of motor disorders, Adv. Funct. Mater. (2019), 1905241.
[15] N. Luo, W. Dai, C. Li, Z. Zhou, L. Lu, C.C.Y. Poon, S.-C. Chen, Y. Zhang, N. Zhao, Flexible piezoresistive sensor patch enabling ultralow power cuffless blood pressure measurement, Adv. Funct. Mater. 26 (2016) 1178–1187.
[16] X. Wang, Y. Gu, Z. Xiong, Z. Cui, T. Zhang, Silk-molded flexible, ultrasensitive, and highly stable electronic skin for monitoring human physiological signals, Adv. Mater. 26 (2014) 1336–1342.
[17] G.Y. Bae, S.W. Pak, D. Kim, G. Lee, D.H. Kim, Y. Chung, K. Cho, Linearly and highly pressure-sensitive electronic skin based on a bioinspired hierarchical structural array, Adv. Mater. 28 (2016), 5300-+.
[18] B. You, C.J. Han, Y. Kim, B.-K. Ju, J.-W. Kim, A wearable piezocapacitive pressure sensor with a single layer of silver nanowire-based elastomeric composite electrodes, J. Mater. Chem. A 4 (2016) 10435–10443.
[19] S.C.B. Mannsfeld, B.C.K. Tee, R.M. Stoltenberg, C.V.H.H. Chen, S. Barman, B.V.O. Muir, A.N. Sokolov, C. Reese, Z. Bao, Highly sensitive flexible pressure sensors with microstructured rubber dielectric layers, Nat. Mater. 9 (2010) 859–864.
[20] V. Sridhar, K. Takahata, A hydrogel-based passive wireless sensor using a flex-circuit inductive transducer, Sens. Actuators A-Phys. 155 (2009) 58–65.
[21] X. Tang, Y. Miao, X. Chen, B. Nie, A flexible and highly sensitive inductive pressure sensor array based on ferrite films, Sensors 19 (10) (2019) 2406.
[22] T. Nguyen Thanh, H. Tran Quang, Y.G. Seoul, D.I. Kim, N.-E. Lee, Physically responsive field-effect transistors with giant electromechanical coupling induced by nanocomposite gate dielectrics, ACS Nano 5 (2011) 7069–7076.
[23] Q. Sun, D.H. Kim, S.S. Park, N.Y. Lee, Y. Zhang, J.H. Lee, K. Cho, J.H. Cho, Transparent, low-power pressure sensor matrix based on coplanar-gate graphene transistors, Adv. Mater. 26 (2014), 4735-+.
[24] L. Pan, A. Chortos, G. Yu, Y. Wang, S. Isaacson, R. Allen, Y. Shi, R. Dauskardt, Z. Bao, An ultra-sensitive resistive pressure sensor based on hollow-sphere microstructure induced elasticity in conducting polymer film, Nat. Commun. 5 (2014).
[25] S. Jung, J.H. Kim, J. Kim, S. Choi, J. Lee, I. Park, T. Hyeon, D.-H. Kim, Reverse-micelle-induced porous pressure-sensitive rubber for wearable human-machine interfaces, Adv. Mater. 26 (2014), 4825-+.
[26] Y. Ding, T. Xu, O. Onyilagha, H. Fong, Z. Zhu, Recent advances in flexible and wearable pressure sensors based on piezoresistive 3D monolithic conductive sponges, ACS Appl. Mater. Interfaces 11 (2019) 6685–6704.
[27] C.-L. Choong, M.-B. Shim, B.-S. Lee, S. Jeon, D.-S. Ko, T.-H. Kang, J. Bae, S.H. Lee, K.-E. Byun, J. Im, Y.J. Jeong, C.E. Park, J.-J. Park, U.I. Chung, Highly stretchable resistive pressure sensors using a conductive elastomeric composite on a micropyramid array, Adv. Mater. 26 (2014) 3451–3458.
[28] C. Pang, G.-Y. Lee, T.-i. Kim, S.M. Kim, H.N. Kim, S.-H. Ahn, K.-Y. Suh, A flexible and highly sensitive strain-gauge sensor using reversible interlocking of nanofibres, Nat. Mater. 11 (2012) 795–801.
[29] G. Schwartz, B.C.K. Tee, J. Mei, A.L. Appleton, D.H. Kim, H. Wang, Z. Bao, Flexible polymer transistors with high pressure sensitivity for application in electronic skin and health monitoring, Nat. Commun. 4 (2013).
[30] B.C.K. Tee, A. Chortos, R.R. Dunn, G. Schwartz, E. Eason, Z. Bao, Tunable flexible pressure sensors using microstructured elastomer geometries for intuitive electronics, Adv. Funct. Mater. 24 (2014) 5427–5434.
[31] B. Su, S. Gong, Z. Ma, L.W. Yap, W. Cheng, Mimosa-inspired design of a flexible pressure sensor with touch sensitivity, Small 11 (2015) 1886–1891.
[32] Y. Wei, S. Chen, Y. Lin, Z. Yang, L. Liu, Cu-Ag core-shell nanowires for electronic skin with a petal molded microstructure, J. Mater. Chem. C 3 (2015) 9594–9602.
[33] P. Nie, R. Wang, X. Xu, Y. Cheng, X. Wang, L. Shi, J. Sun, High-performance piezoresistive electronic skin with bionic hierarchical microstructure and microcracks, ACS Appl. Mater. Interfaces 9 (2017) 14911–14919.
[34] M. Hopkins, R. Vaidyanathan, A.H. McGregor, Examination of the performance characteristics of velostat as an in-socket pressure sensor, IEEE Sens. J. 20 (2020) 6992–7000.
[35] A. Chortos, Z. Bao, Skin-inspired electronic devices, Mater. Today 17 (2014) 321–331.

Biographies

Hao Tang received his Bachelor of Engineering in 2017 from Hebei University of technology. Currently, he is studying as a PhD candidate at Shanghai Institute of Ceramics, Chinese Academy of Science. His research topic is flexible and stretchable electronic device.

Pu Nie received his Bachelor of Engineering in 2014 from Nanjing University of Technology. And he obtained his master degree in 2017 from Shanghai Institute of Ceramics, Chinese Academy of Science. His research topic is flexible pressure sensors.

Ranran Wang, Associate professor from Shanghai Institute of Ceramics, Chinese Academy of Science. Her research activity concerns with low dimensional flexible electronic materials and flexible wearable electronic devices.

Jing Sun, Professor from Shanghai Institute of Ceramics, Chinese Academy of Science. Her research activity focuses on preparation of flexible wearable electronic devices and photocatalytic degradation of typical atmospheric VOCs.